Article

Aromatic vs Aliphatic C–H Bond Activation by Rhodium(I) as a Function of Agostic Interactions: Catalytic H/D Exchange between Olefins and Methanol or Water

Boris Rybtchinski, Revital Cohen, Yehoshoa Ben-David, Jan M. L. Martin, and David Milstein

J. Am. Chem. Soc., **2003**, 125 (36), 11041-11050• DOI: 10.1021/ja029197g • Publication Date (Web): 14 August 2003

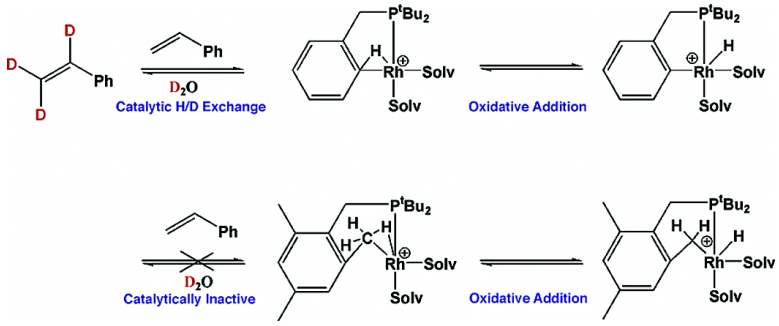

More About This Article

Additional resources and features associated with this article are available within the HTML version:

- Supporting Information
- Links to the 17 articles that cite this article, as of the time of this article download
- Access to high resolution figures
- Links to articles and content related to this article
- Copyright permission to reproduce figures and/or text from this article

View the Full Text HTML

J|A|C|S
ARTICLES
Published on Web 08/14/2003

Aromatic vs Aliphatic C−H Bond Activation by Rhodium(I) as a Function of Agostic Interactions: Catalytic H/D Exchange between Olefins and Methanol or Water

Boris Rybtchinski, Revital Cohen, Yehoshoa Ben-David, Jan M. L. Martin,* and David Milstein*

Contribution from the Department of Organic Chemistry, The Weizmann Institute of Science, 76100 Rehovot, Israel

Received November 3, 2002; Revised Manuscript Received May 29, 2003; E-mail: david.milstein@weizmann.ac.il; comartin@wicc.weizmann.ac.il

Abstract: The aryl−PC type ligand **3**, benzyl(di-*tert*-butyl)phosphane, reacts with $[Rh(coe)_2(solv)_n]BF_4$ (coe = cyclooctene, solv = solvent), producing the C−H activated complexes **4a**−**c** (solv = (**a**) acetone, (**b**) THF, (**c**) methanol). Complexes **4a**−**c** undergo reversible arene C−H activation (observed by NMR spin saturation transfer experiments, SST) and H/D exchange into the hydride and aryl *ortho*-H with ROD (R = D, Me). They also promote catalytic H/D exchange into the vinylic C−H bond of olefins, with deuterated methanol or water utilized as D-donors. Unexpectedly, complex **2**, based on the benzyl-PC type ligand **1** (analogous to **3**), di-*tert*-butyl(2,4,6-trimethylbenzyl)phosphane, shows a very different reversible C−H activation pattern as observed by SST. It is not active in H/D exchange with ROD and in catalytic H/D exchange with olefins. To clarify our observations regarding C−H activation/reductive elimination in both PC−Rh systems, density functional theory (DFT) calculations were performed. Both nucleophilic (oxidative addition) and electrophilic (H/D exchange) C−H activation proceed through η^2-C,H agostic intermediates. In the aryl-PC system the agostic interaction causes C−H bond acidity sufficient for the H/D exchange with water or methanol, which is not the case in the benzyl PC−Rh system. In the latter system the C−H coordination pattern of the methyl controls the reversible C−H oxidative addition leading to energetically different C−H activation processes, in accordance with the experimental observations.

Introduction

Mechanistic studies of C−H activation by late transition metals revealed a number of important characteristics of this process.[1] Jones and Feher inferred from competition experiments and kinetic isotope effects that coordination of benzene at $Cp^*Rh(PMe_3)$ lowers the barriers to C−H activation.[2] The η^2-C,C benzene intermediate in the course of C−H activation was first observed by Perutz et al.[3a] and was characterized in solution and shown to be at equilibrium with aryl hydride complexes.[3,4] Such an intermediate was recently isolated and shown to undergo facile C−H activation; X-ray and NMR evidence for η^2-C,C coordination during the reaction was provided.[5] The importance of η^2-C,H coordination was also demonstrated, and C−H activation in arenes may proceed through such complexes without the direct involvement of η^2-C,C intermediates.[6−8] In the case of aliphatic C−H bond activation, a growing body of evidence suggests that C−H bond coordination to a metal center precedes the bond cleavage step in virtually all cases.[1] It is generally recognized that C−H bond activation in aromatic hydrocarbons is favored over the aliphatic ones due to kinetic (η^2-C,C arene coordination) and thermodynamic (strong M−aryl bond) factors.[1] An important consequence of agostic bonding and η^2-C,H bonding in general is the increased acidity of the C−H bond due to the donation from C−H bond σ orbital to a metal center.[1b] In a few cases this leads to facile deprotonation[8] and H/D exchange with D_2O.[8a] As aliphatic σ complexes[9] draw great attention in view of their relevance to saturated hydrocarbon activation, aromatic η^2-C,H σ-bonding is less studied.

(1) (a) Crabtree, R. H. *Chem. Rev.* **1985**, *85*, 245. (b) Crabtree, R. H. *J. Chem. Soc., Dalton Trans.* **2001**, 2437. (c) Shilov, A. E.; Shul'pin, G. B. *Chem. Rev.* **1997**, *97*, 2879. (d) Arndtsen, B. A.; Bergman, R. G.; Mobley, T. A.; Peterson, T. H. *Acc. Chem. Res.* **1995**, *28*, 154. (e) Labinger, J. A, Bercaw, J. E. *Nature* **2002**, *417*, 507.

(2) For a review, see: Jones, W. D.; Feher, F. J. *Acc. Chem. Res.* **1989**, *22*, 91.

(3) (a) Belt, S. T.; Duckett, S. B.; Helliwell, M.; Perutz, R. N. *J. Chem. Soc., Chem. Commun.* **1989**, 928. (b) Belt, S. T.; Dong, L.; Duckett, S. B.; Jones, W. D.; Partridge, M. G.; Perutz, R. N. *J. Chem. Soc., Chem. Commun.* **1991**, 266. (c) Chin, R. M.; Dong, L.; Duckett, S. B.; Partridge, M. G.; Jones, W. D.; Perutz, R. N. *J. Am. Chem. Soc.* **1993**, *115*, 7685.

(4) Johansson, L.; Tilset, M.; Labinger, J. A.; Bercaw, J. E. *J. Am. Chem. Soc.* **2000**, *122*, 10846.

(5) Reinartz, S.; White, P. S.; Brookhart, M.; Templeton, J. L. *J. Am. Chem. Soc.* **2001**, *123*, 12724.

(6) Aromatic C−H activation proceeding directly through η^2-C,H adducts: (a) Peterson, T. H.; Golden, J. T.; Bergman, R. G. *J. Am. Chem. Soc.* **2001**, *123*, 455. (b) Asplund, M. C.; Snee, P. T.; Yeston, J. S.; Wilkens, M. J.; Payne, C. K.; Yang, H.; Kotz, K. T.; Frei, H.; Bergman, R. G.; Harris, C. B. *J. Am. Chem. Soc.* **2002**, *124*, 10605.

(7) Aromatic C−H oxidative addition proceeding directly through η^2-C,H agostic complexes: (a) Lavin, M.; Holt, E. M.; Crabtree, R. H. *Organometallics* **1989**, *8*, 99. (b) Toner, A. J.; Grundemann, S.; Clot, E.; Limbach, H.-H.; Donnadieu, B.; Sabo-Etienne, S.; Chaudret, B. *J. Am. Chem. Soc.* **2000**, *122*, 6777.

(8) Aromatic C−H activation proceeding by deprotonation of η^2-C,H agostic complexes: (a) Vigalok, A.; Uzan, O.; Shimon, L. J. W.; Ben-David, Y.; Martin, J. M. L.; Milstein, D. *J. Am. Chem. Soc.* **1998**, *120*, 12539. (b) Gusev, D. G.; Madott, M.; Dolgushin, F. M.; Lyssenko, K. A.; Antipin, M. Y. *Organometallics* **2000**, *19*, 1734.

(9) Hall, C.; Perutz, R. N. *Chem. Rev.* **1996**, *96*, 3125.

10.1021/ja029197g CCC: $25.00

Scheme 1

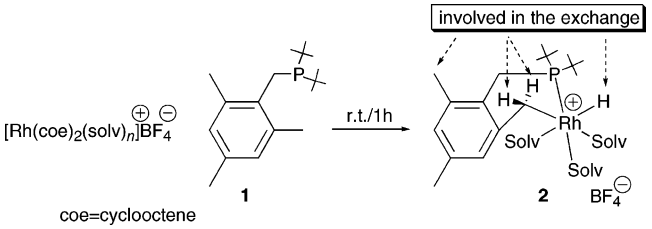

Scheme 2

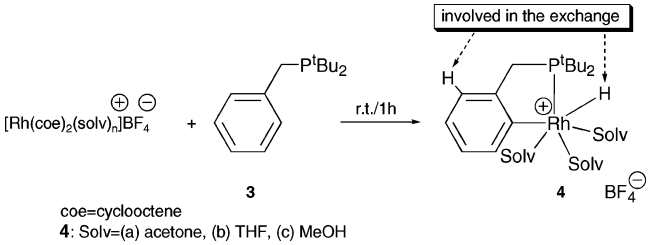

We have recently reported a system that exhibits an intriguing mode of reversible C−H activation (Scheme 1).[10] In this system the reversible C−H bond elimination proceeds in a stepwise manner with increasing the temperature. Spin saturation transfer experiments involving selective irradiation of the hydride ligand revealed that initially only one hydrogen atom of the methylene bridge, Rh−CH_2−aryl, is involved in the exchange, and then upon temperature increase the two methylene protons are exchanged and with further temperature increase the *ortho* methyl protons start to exchange (Scheme 1). We suggested that agostic bonding might be responsible for this behavior. Complex **2** did not show any H/D exchange with deuterated solvents (THF, acetone, methanol, water).

We now report on a PC−Rh system based on the ligand **3**, which exhibits behavior in cyclometalation and H/D exchange with ROH (R = H, Me) very different from that of complex **2**. Moreover, this system promotes catalytic H/D exchange into olefins with MeOD and D_2O. To clarify the observed reactivity, we performed a computational DFT study of the C−H activation process in both aliphatic (based on ligand **1**) and aromatic (based on ligand **3**) PC−Rh systems. The differences in agostic η^2-C,H bonding were found to account for the observed striking reactivity difference between the two systems.

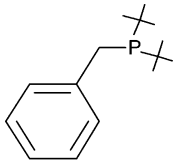

3

Experimental Results

Cationic rhodium(I) precursors, $[Rh(coe)_2(solv)_n]BF_4$ (coe = cyclooctene, solv = solvent), were obtained by chloride abstraction from $[Rh(coe)_2Cl]_2$, according to a known procedure.[11] When $[Rh(coe)_2(solv)_n]BF_4$ was reacted at room temperature with the ligand **3** in THF, acetone, or methanol, quantitative formation of the C−H activation products **4a**−**c**, respectively, was observed within 1 h (Scheme 2). Evaporation and redissolving in a polar solvent of choice resulted in the clean compounds **4a**−**c**, which were characterized by NMR (complex **4c** also by elemental analysis and MS) and possess similar spectral characteristics. For example complex **4c** gives rise to a broad doublet centered at 109.82 ppm ($^1J_{RhP}$ = 175.8 Hz) in $^{31}P\{^1H\}$ NMR. The Rh−*H* signal appears as a doublet of doublets at −22.66 ppm ($^1J_{RhH}$ = 33.2 Hz, $^2J_{PH}$ = 26.5 Hz) in ^1H NMR. The aromatic *ipso* carbon gives rise to a broad doublet centered at 150.40 ppm ($^1J_{RhC}$ = 36.8 Hz) in the $^{13}C\{^1H\}$ NMR spectrum. All the compounds are stable in polar solvents and slightly soluble in water. An acetone−water mixture (5:1 v/v) is an excellent solvent.

Spin saturation transfer (SST) experiments involving selective irradiation of the hydride ligand in **4a**−**c** at 23 °C indicated chemical exchange between the hydride and the *ortho* proton (Scheme 2). Quantitative SST analysis of the exchange processes in complex **4** is hampered by the fact that solvent dissociation precedes the C−H elimination step.[12] Comparing SST in complexes **2c** and **4c** (methanol as a solvent) revealed that under the same conditions (23 °C) complex **2c** (Scheme 1) exhibited exchange involving only one proton of the methylene group. Exchange with the second methylene proton and *ortho* methyl group started to take place only at higher temperatures. This is a surprising observation, in view of the expected easier C−H reductive elimination of **2** due to the weaker Rh−benzyl as compared with Rh−aryl bonds and the more stable five- vs six-membered chelate.

A striking difference between complexes **2** and **4** was observed also regarding H/D exchange phenomena. Thus, complex **2** did not show any H/D exchange in MeOD or D_2O at room temperature or upon heating. Yet, H/D exchange took place in complex **4** in CD_3OD, completely substituting the hydride and the aromatic *ortho*-hydrogen atom for D within 24 h at room temperature (or within 2 h at 65 °C). Since the methanol CD_3 group remained intact and no formaldehyde or carbonyl complexes were observed, only the deuterium atoms of the O−D group are responsible for the exchange. In acetone-d_6 and THF-d_8 no significant H/D exchange took place. Significantly, the acetone−water system is similar to methanol both in SST and H/D exchange (hydride and *ortho*-H exchange takes place when D_2O is used), confirming that the O−D group is critical for the exchange. As both complexes **2** and **4** are hydrides, and in both of them coordinated methanol or water molecules are present, the H/D exchange in **4** is unlikely to proceed through a process involving the hydride, by a $H^{\delta-}\cdots H^{\delta+}$ type interaction.[13] Moreover, if $H^{\delta-}\cdots H^{\delta+}$ type interaction were responsible for the H/D exchange, it would be more facile in the case of **2** which is slightly more hydridic. We explain the

(10) Rybtchinski, B.; Konstantinovsky, L.; Shimon, L. J. W.; Vigalok, A.; Milstein, D. *Chem. Eur. J.* **2000**, *17*, 3287.
(11) Schrock, R. R.; Osborn, J. A. *J. Am. Chem. Soc.* **1971**, *93*, 3089.
(12) We performed quantitative analysis of the exchange rate constants in complex **2** in various solvents and at various temperatures (see ref 10). It was found that the constants are representative of a complex process involving solvent dissociation. Our computational results support this conclusion. Thus, the C−H reductive elimination/oxidative addition mechanism in complexes **2** and **4** appears to be difficult to assess by SST quantitative analysis (although in complex **2** rates of *various exchange processes* can be compared).
(13) For an Ir−H/N−H exchange postulated to proceed via an $H^{\delta-}\cdots H^{\delta+}$ interaction, see: Koelliker, R.; Milstein, D. *J. Am. Chem. Soc.* **1991**, *113*, 8524.

Table 1. Relative Energies (ΔE_e) and Free Energies (ΔG_{298}) of the Various Complexes of the Aryl− and Benzyl−PC/Rh Systems at the mPW1k/SDB-cc-pVDZ//mPW1k/SDD Level of Theory

complex	ΔE_e (kcal/mol)	ΔG_{298} (kcal/mol)
Aryl−PC/Rh System		
Me-CHactiv3MeOH (**5**)	0.00	0.00
Me-CH-activated (**6** + MeOH)	21.59	7.59
Me-CH-agostic (**7** + MeOH)	24.45	11.10
Me-CC-Eta2 (**8**,**8**enant + MeOH)	21.02	9.67
Me-openArm-3MeOH (**9**)	4.65	4.51
Me-TS-CHagostic-to-CHactivated (TS(**6**−**7**) + MeOH)	26.73	12.07
Me-TS-Agostic-to-Eta2 (TS(**7**−**8**) + MeOH)	28.22	14.87
Me-TS-Eta2-to-Eta2(enantiomer) (TS(**8**,**8**enant) + MeOH)	25.10	12.69
Me-TS-openArm3MeOH to Agostic2MeOH (TS(**7**−**9**))	20.45	19.11
Benzyl−PC/Rh System		
Me-CHactivated-3MeOH-exo (**10**)	0.00	0.00
Me-CHactivated-3MeOH-endo (**10***)	5.13	5.24
Me-CHactivated-2MeOH-exo (**11** + MeOH)	23.05	8.73
Me-CHactivated-2MeOH-endo (**11*** + MeOH)	25.95	12.19
Me-CH-agostic-exo (**12** + MeOH)	33.14	19.97
Me-CH-agostic-endo (**12*** + MeOH)	29.96	17.70
Me-CC-Eta2 (**13** + MeOH)	26.47	15.15
Me-openArm3MeOH (**14**)	8.57	9.30
Me-TS-CHagostic-to-CHactivated-exo (TS(**12**−**11**) + MeOH)	35.73	21.43
Me-TS-CHagostic-to-CHactivated-endo (TS(**12***−**11***) + MeOH)	34.83	21.26
Me-TS-Agostic-Exo-to-Agostic-Endo (TS(**12**−**12***) + MeOH)	33.36	21.91
Me-TS-CH3-in-place-rotation (TS(**12**−**12**) + MeOH)	36.79	23.71
Me-TS-CHagostic-to-CC-Eta2 (TS(**12**−**13**) + MeOH)	36.89	24.02
Me-TS-Eta2-to-Eta2(enantiomer) (TS(**13**−**13**enant)+ MeOH)	28.13	16.50
Me-TS-openArm3MeOH-to-Eta22MeOH (TS(**14**−**13**))	25.84	25.22

Scheme 3

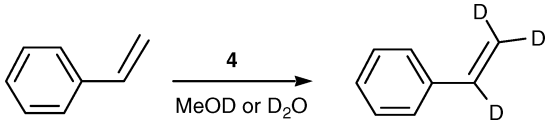

H/D exchange phenomena in terms of stronger aromatic C−H agostic interactions in the case of **4**. This interaction increases the C−H bond acidity significantly, sufficiently to promote H/D exchange with weak acids such as D_2O and MeOD (see Computational Results and Discussion). Reaction of **4** with bases (KOtBu, NEt_3) leads to decomposition.

Vinylic H/D Exchange in Olefins. Complex **4** catalyses H/D exchange of the vinylic protons of styrene in the presence of D_2O or MeOD at 60 °C (Scheme 3). *Exclusive vinylic H/D exchange is observed, no other protons being substituted by deuterium.* In methanol a catalytic H/D exchange process with about 80% exchange and 50 TON takes place after heating for 24 h at 60 °C. Similar reactivity and TON were observed using acetone/D_2O (5:1 v/v, respectively) mixture. Notably, complex **2** does not catalyze H/D exchange with olefins under the same conditions.

Other terminal olefins such as *tert*-butylethylene and (trimethylsilyl)ethylene also show H/D exchange, the process being slower and less efficient than that with styrene. Internal olefins such as cyclooctene and cyclohexene do not undergo exchange. Reversible olefin insertion into Rh−H bond coupled with the H/D exchange in **4** described above can be responsible for the observed phenomena. The intimate mechanism and scope of the olefin deuteration is under current investigation. It should be noted that general procedures utilizing D_2O for the incorporation of deuterium into organic compounds are often limited to activated positions.[14] Only in a few cases unactivated organic compounds were deuterated utilizing D_2O in the presence of a transition metal catalyst[15,16] To the best of our knowledge selective H/D exchange of olefins with D_2O or MeOD catalyzed by metal complex has not been described. Such a process can be useful for the synthesis of selectively deuterated olefins.

Computational Results

To clarify our observations regarding C−H activation/reductive elimination, density functional theory (DFT) calculations were performed at the mPW1k/SDB-cc-pVDZ//mPW1k/SDD level of theory. Calculations were carried out first for the aromatic and aliphatic PC system with H substituents on the phosphines (H−PC systems) to reduce the computational time. Afterward, the calculations were performed for the Me−PC−Rh systems (using H−PC geometries as a starting point) to identify plausible reaction pathways. Methyl substituents on the phosphine were chosen as the ones mimicking ^{t}Bu in their electronic properties and rendering the computational time reasonable. In the experimental aliphatic PC system the *para*-Me group is not involved in the interaction with the metal center; thus, only the two Me groups *ortho* to the phosphine arm were introduced in the computational model system. A summary of the computational results is given in Table 1. We chose the C−H activation products, complexes **5** and **10,** as reference zero points as these complexes correspond to the ones observed experimentally and are the most stable species. It should be noted that these complexes have 3 bound MeOH molecules while the reaction intermediates have only 2 MeOH molecules bound to the metal center. Thus, the relative energies of the intermediates do include the solvent binding energy and

(14) For recent review on H/D exchange involving C−H activation see: (a) Junk, T.; Catallo, W. J. *Chem. Soc. Rev.* **1997**, *26*, 401. See also ref 1b.

(15) K_2PtCl_4 was reported to catalyze exchange in arenes and alkanes: (a) Garnett, J. L.; Hodges, R. J. *J. Am. Chem. Soc.* **1967**, *89*, 4546. (b) Shilov, A. E.; Shteinman, A. A. *Coord. Chem. Rev.* **1977**, *24*, 97.

(16) Cp*(PMe_3)$IrCl_2$ catalyzes H/D exchange utilizing D_2O in a variety of organic substrates: Klei, S. R.; Golden, J. T.; Tilley, T. D.; Bergman, R. G. *J. Am. Chem. Soc.* **2002**, *124*, 2092.

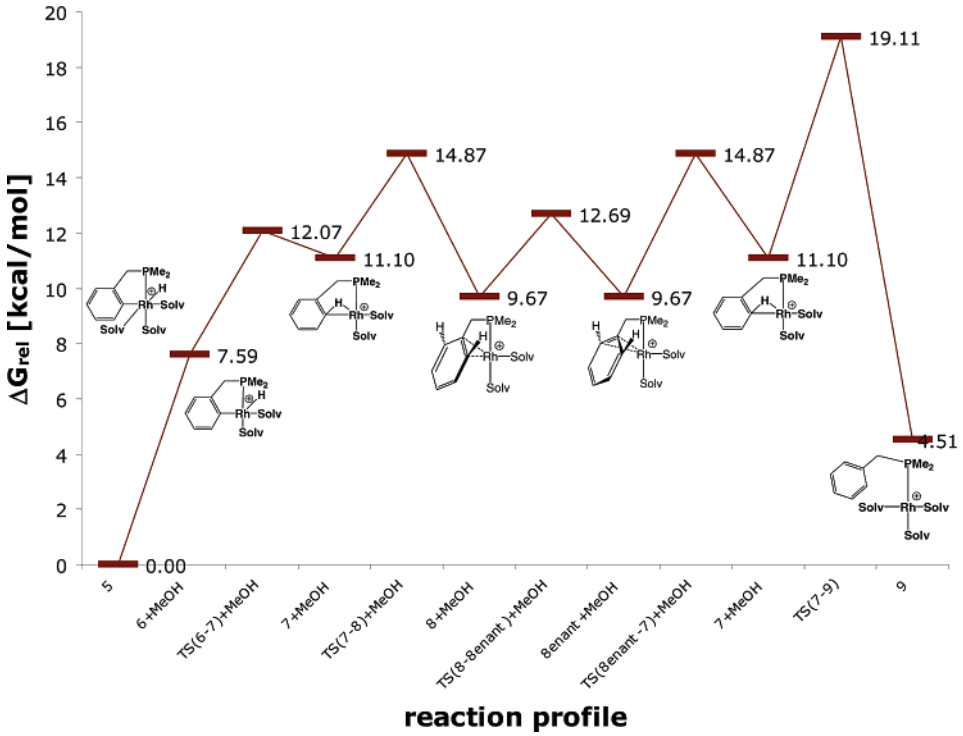

Figure 1. . Aryl−(Me)PC/Rh system: Reaction profile (ΔG_{298}) for C−H activation and exchange at the mPW1k/SDB-cc-pVDZ//mPW1k/SDD level of theory.

Scheme 4

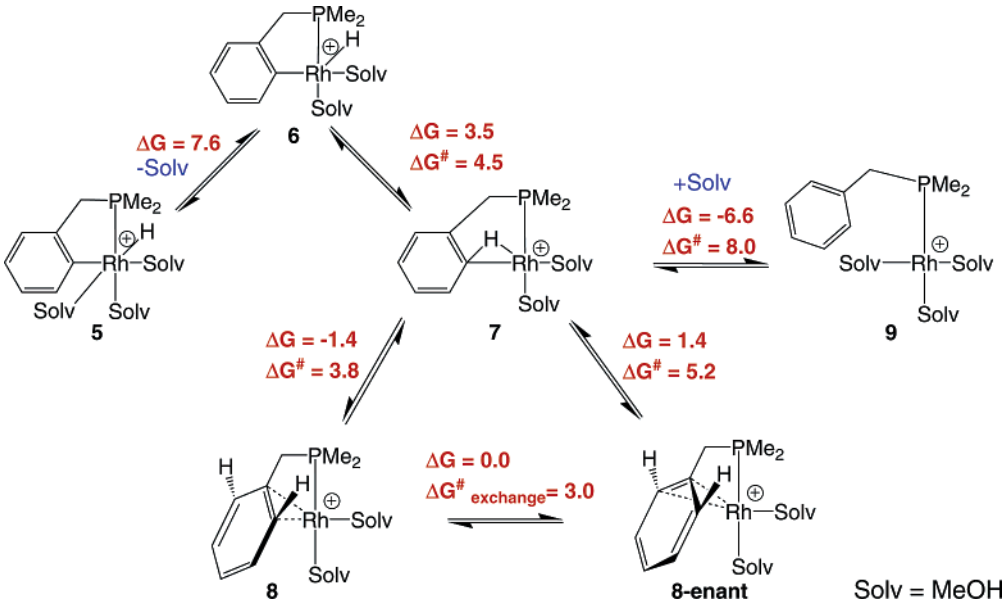

therefore are high in energy relative to the starting compound. The free energy (ΔG_{298}) values, unlike the ΔE_e values, include the variation in entropy as obtained from the thermal corrections calculated using the rigid rotor harmonic oscillator approximation.

Aromatic Me−PC/Rh System. The reaction pathway found for the aromatic system is presented in Scheme 4 and Figure 1.

The lowest energy pathway proceeds through species with two (intermediates) or three (products) coordinated methanol molecules. A pathway involving only one coordinated methanol molecule was found to be much higher in energy.

The C−H reductive elimination path starts with dissociation of a methanol molecule from **5** to produce **6**, which is 7.6 kcal/mol higher in free energy. Subsequently, **6** undergoes reductive elimination, with a barrier of 4.5 kcal/mol, to form an agostic intermediate **7**.[17] Then formation of an η^2-aryl complex **8** takes place with a barrier of 3.8 kcal/mol. Complex **8** can rearrange to its enantiomer **8**-enant ($\Delta G^{\ddagger} = 3$ kcal/mol). This interconversion opens a channel for an exchange between the hydride and the *ortho* hydrogen atom.[18] The barriers of all the processes are relatively low (see Scheme 4 and Figure 1), in agreement with the experimental observation of the hydride/*ortho*-H

(17) A high-energy process (barrier of 15.8 kcal/mol), involving concerted C−H reductive elimination and MeOH loss to form **5** directly from **7**, was also found.

(18) No exchange pathway involving rotation of the Ph ring was found to take place directly from the agostic complex **7**.

Scheme 5

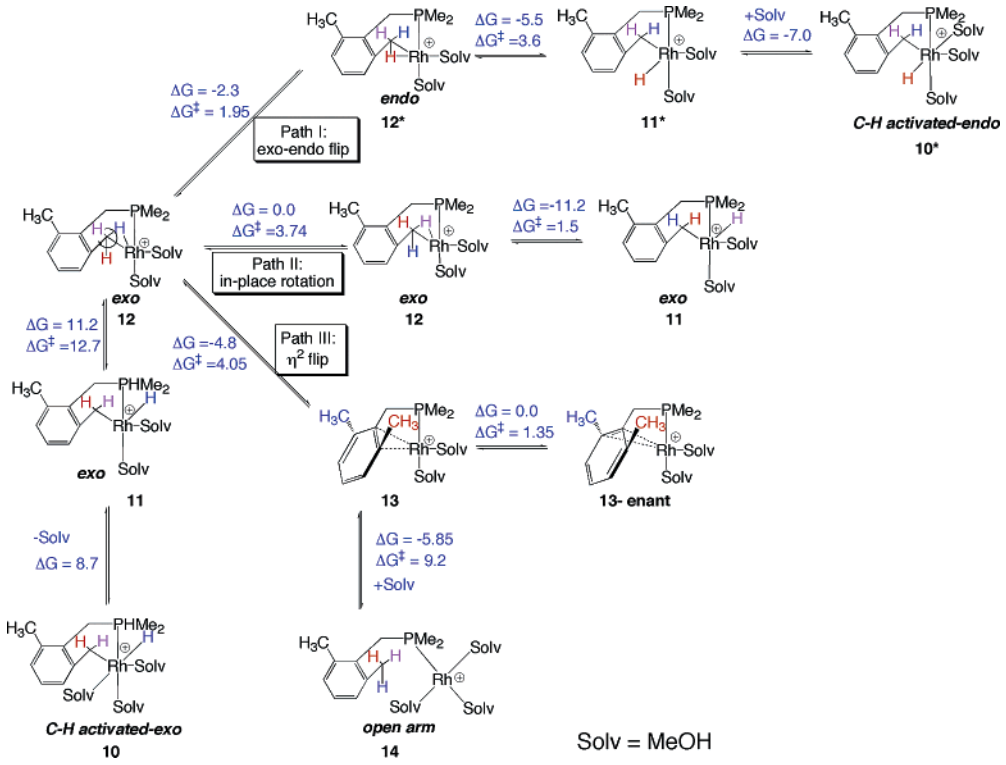

exchange at room temperature. Complete opening of the system to give **9** appears to be a less favorable pathway for this exchange ($\Delta G^{\ddagger} = 8$ kcal/mol).[19,20]

Aliphatic Me−PC/Rh System. Similarly to the aromatic system the lowest energy pathways proceed through species with two or three coordinated methanol molecules (the path with one coordinated methanol molecule was found to be much higher in energy). However, in contrast to the aromatic systems, the aliphatic one allows a variety of possible geometries in the course of the C−H reductive elimination/activation (Scheme 5).

The main difference between the aliphatic system and its aromatic counterpart is higher barriers for the reductive elimination process from the Rh(III) hydride to the Rh(I) C−H agostic complex, $\Delta G^{\ddagger}_{RE} = 12.7$ in the aliphatic system vs 4.5 kcal/mol in the aromatic one. This is in agreement with the experimentally observed exchange selectivity in the aliphatic system (complex **2c**) in which not all the processes responsible for the observed reversible C−H activation pattern can happen at room temperature. We found two isomers for the C−H activation product: *exo* and *endo*, complexes **10** and **10*** respectively. Complex **10** is more stable and most probably corresponds to the experimentally observed complex **2c**. All the agostic complexes found computationally also have *endo* and *exo* isomers, and the pathways accounting for the exchange processes were found to proceed through these agostic intermediates.

Three different pathways were found (Scheme 5, Figure 2) for the exchange reactions corresponding to the experimentally observed SST phenomena (exchange between Rh−*H*, Rh−CH_2−aryl and *ortho* CH_3−aryl). Pathway I involves an "*exo-endo ring flip*" reaction, which allows the exchange of the hydride with only one hydrogen of the Rh−CH_2−aryl group. The flip between the *exo* and the *endo* conformations (**12** and **12***, respectively) is followed by C−H oxidative addition in **12*** to form the *endo* isomer **11***. In this pathway only one of the Rh−CH_2−aryl protons is geometrically preferable for the exchange (see below). Pathway II involves an "*in-place rotation*" process of the methyl group bound in an *exo*-agostic mode to the Rh center in complex **12**. This process has a 1.8 kcal/mol higher energy barrier than the ring flip process. Pathway III, *η^2-flip*, involves a conversion between the *exo*-agostic complex **12** and the η^2-C,C aryl one **13**. Complex **13** can be converted to its enantiomer **13**-enant, opening a channel to the C−H activation in the *ortho*-Me group (Scheme 5, Figure 2).

As the barrier of the *exo-endo* flip, pathway I, is slightly lower than that of the in-place rotation of the Me group, pathway II ($\Delta G^{\ddagger} = 1.95$ vs 3.7 kcal/mol), the selective exchange can take place. The kinetic barrier of the η^2-flip reaction was found to be comparable to that of the Me in-place rotation ($\Delta G^{\ddagger} = 4.05$ vs 3.7 kcal/mol). However, in **12** two C−H bonds are available for bonding to the metal center in the course of Me in-place rotation upon clockwise and counterclockwise motion. On the other hand, only one arene C−C bond, which is situated between the agostic Me and the phosphine arm in **12**, is available for η^2-C,C bonding. Therefore, the rate of Me rotation should be increased by approximately a factor of 2. The tendency in the DFT computed reaction pathways (the rates increase in the order I < II < III) fits the selectivity observed experimentally. It should be noted that the experimentally observed SST selectivity in **2c** is in the temperature range of 13 °C,[10] implying that the difference in the kinetic barriers is small, in good agreement with the computed small differences between the reaction

(19) The value of $\Delta G^{\ddagger}$ for this barrier is probably underestimated due to hydrogen bonding in the TS between the H atom of the dissociated methanol and the O atom of the coordinated methanol.

(20) No analogue of **9** with two coordinated MeOH molecules was found. Repeated attempts to locate this minimum resulted in the convergence to **8**.

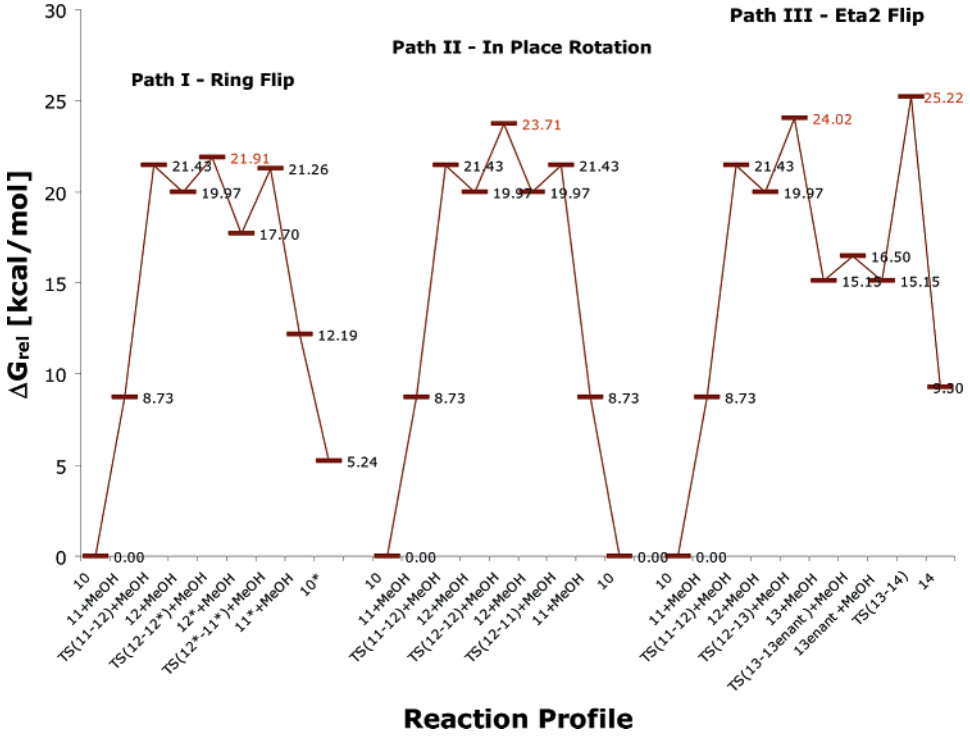

Figure 2. **.** Benzyl−(Me)PC/Rh system: Three reaction profiles (ΔG_{298}) for C−H activation and exchange at the mPW1k/SDB-cc-pVDZ//mPW1k/SDD level of theory.

barriers. In addition, the experimentally found ratio for the exchange of one and two methylene protons ($k_{2H}/k_{1H} = 1/20$),[10] which translates to a barrier difference of 1.8 kcal/mol, is in excellent agreement with the one found computationally for the *exo-endo* flip path and in-place rotation ($\Delta\Delta G^{\ddagger} = 1.8$ kcal/mol). Thus, pathway I (*exo-endo* flip) leads to the selective exchange of only one methylene proton at room temperature, pathway II (in-place rotation) to the exchange of the two methylene protons at slightly elevated temperatures and pathway III (η^2-flip) to the exchange at higher temperatures with the second *ortho*-methyl group.

Significantly, distinctively different reactivity is found for *endo* and *exo* isomers. We found that most of the productive exchange phenomena proceed through the agostic *exo*-isomer **12**. It should be noted that, in addition to the agostic C−H in complex **12***, another C−H bond of the agostically bound Me group appears to be involved in the interaction with the metal center. Although this interaction seems to be rather weak (Figure 3, Table 2), it is a noticeable one in **12*** and absent in **12**. This interaction may account for the higher stability (by 2.3 kcal/mol) of **12*** in comparison to **12**. Neither in-place rotation nor η^2-C,C coordination was found to start from the *endo* isomer **12***, the only productive pathways being C−H activation and isomerization into *exo*-isomer **12**. Thus, the specific geometry of the η^2-C,H bound Me group in **12*** predisposes one of the nonagostic C−H bonds to the interaction with the metal center. It is in line with our previous suggestion[10] and can account for the selective exchange phenomena in **2c** (see below).

Structure of the Agostic Complexes. An important feature of both the aromatic and aliphatic PC−Rh systems is that the agostic intermediates are consistently found in all the pathways involving C−H reductive elimination/activation. Since they appear to be the key intermediates in these processes, we present here a comparison of their characteristics. Bond lengths and Wiberg NBO (natural bond orders) of **7**, **12**, and **12*** are given in Table 2, and optimized structures are presented is Figure 3. The geometry of the metal−C−H agostic triangles (Figure 3, Table 2) indicates that the rhodium center is situated closer to the arene C−H bond in **7** than to that of the CH_3 group in **12** or **12***, indicative of stronger agostic bonding in **7**.[21] Bond order analysis (Table 2) further confirms a higher degree of bonding between the metal center and the arene C−H. There is also a noticeable predisposition to bonding of one of the nonagostic H of the Me group. Significantly, analysis of the partial charges reveals that in the aliphatic case (**12** and **12***) the agostically bound H acquires some hydridic character (partial charge of +0.198 on agostic H atom vs +0.246 to +0.278 for the other methyl H atoms[22]), whereas in the aromatic case the electron density on the agostic H atom slightly decreases (partial charge of +0.241 on the agostic H atom vs +0.220 to +0.240 for the other aromatic H atoms).[23] In **12** and **12*** the metal is bound tightly to agostic H and is relatively remote from the agostic carbon; in **7** the metal is situated close to both the C and H atoms of the agostic bond. It is in accordance with the metal trajectory in the agostic bonding derived by Crabtree et al.: the stronger the agostic bond, the shorter an M−C bond is observed and vice versa.[21] Stronger agostic bonding in **7** may be a consequence of various factors: involvement of the aromatic ring π-system in the agostic C−H bonding;[23] chelating ring size differences; better polarizability of the sp^2 vs sp^3 hybridized orbital. It appears that due to strong agostic bonding in **7**, the C−H bond becomes sufficiently acidic to exchange with water

(21) Crabtree, R. H.; Holt, E. M.; Lavin, M.; Morehouse, S. M. *Inorg. Chem.* **1985**, *24*, 1986.
(22) Natural population analysis (NPA) [ref 45].
(23) A slightly arenium character of **7** is demonstrated by the bond lengths and bond orders alternation in the aromatic ring, although most of the positive charge is still localized on the metal center, similarly to the system reported in ref 8a.

Table 2. Bond Angles (deg) Bond Lengths (Å) and Bond Orders of the Agostic Complexes in Aryl− and Benzyl−PC/Rh Systems at the mPW1k/SDD Level of Theory

	7		12		12*	
bond angles	Rh−H1−C2	98.24	Rh−H1−C4	113.21	Rh−H3−C4	106.99
	Rh−C2−H1	51.40	Rh−C4−H1	41.29	Rh−C4−H3	45.69
	C7−C2−C3	120.07	Rh−C4−C5	96.96	Rh−C4−C5	126.02
	C5−C6−C7	120.49	C6−C5−C10	119.70	C6−C5−C10	119.86
	C7−C2−H1	119.85	C8−C7−C11	119.03	C8−C7−C11	119.14
	C5−C6−H8	119.67	Rh−C4−H3	94.30	Rh−C4−H1	70.54
	C6−C7−C2−H1	159.12	C9−C8−C7−C11	178.83	C9−C8−C7−C11	179.04
	C4−C5−C6−H8	179.00	C7−C6−C5−C4	174.73	C7−C6−C5−C4	−178.27
bond lengths	Rh−C2	2.259	Rh−C4	2.455	Rh−C4	2.398
	Rh−H1	1.784	Rh−H1	1.763	Rh−H3	1.794
	C2−H1	1.154	Rh−H2	3.334	Rh−H1	2.280
	C6−H8	1.079	Rh−H3	2.757	Rh−H2	3.071
	C2−C3	1.398	C4−H1	1.150	C4−H1	1.094
	C3−C4	1.393	C4−H2	1.095	C4−H3	1.151
	C4−C5	1.395	C4−H3	1.085	C4−H2	1.086
	C5−C6	1.397				
	C6−C7	1.393				
	C7−C2	1.410				
bond orders	Rh−C2	0.253	Rh−C4	0.179	Rh−C4	0.184
	Rh−H1	0.144	Rh−H1	0.128	Rh−H3	0.127
	C2−H1	0.746	Rh−H2	0.014	Rh−H1	0.021
	C6−H8	0.908	Rh−H3	0.003	Rh−H2	0.009
	C2−C3	1.341	C4−H1	0.788	C4−H1	0.887
	C3−C4	1.421	C4−H2	0.873	C4−H3	0.783
	C4−C5	1.423	C4−H3	0.92	C4−H2	0.904
	C5−C6	1.436				
	C6−C7	1.442				
	C7−C2	1.398				

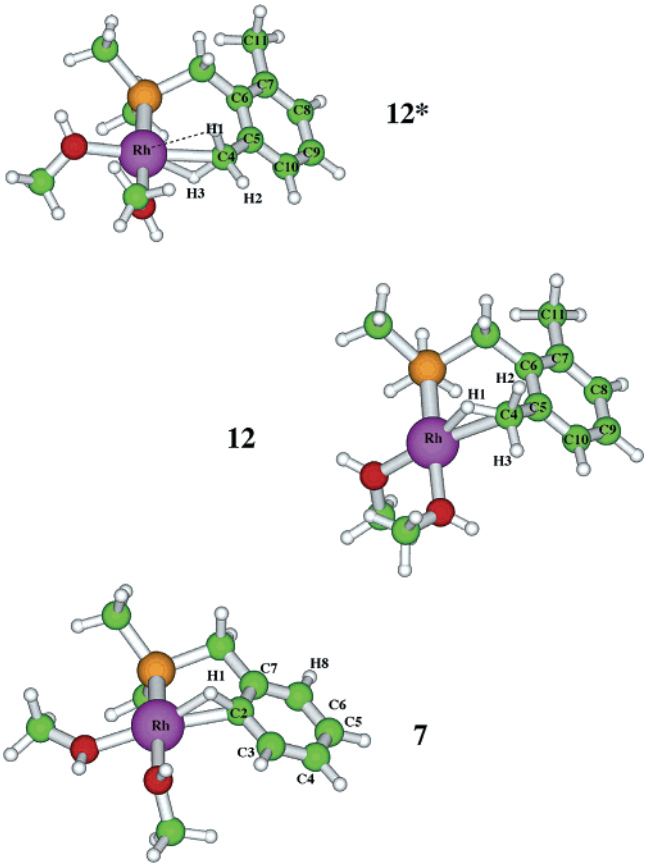

Figure 3. . Optimized geometries of the agostic complexes: **7**, **12** (*exo*), and **12*** (*endo*) as obtained at the mPW1k/SDD level of theory.

and methanol in a way resembling a previously reported (PCP)-Rh(CO)$^+$ system.[8a] In the case of **12** the agostic C−H appears to be less acidic and does not exchange with D_2O and MeOD. Thus, both agostic complexes **7** and **12** (**12***) can lead to the C−H bond oxidative addition, but only the arene C−H agostic bonding in **7** results in high C−H bond acidification (see Discussion).

Discussion

Control of C−H Oxidative Addition and Reductive Elimination by η^2-C,H Coordination: PC−Rh Systems.

The proposed two-step model[24] describes the metal/C−H oxidative addition as follows. The first step, coordination, involves forward donation from a C−H bonding σ orbital to a vacant metal-based orbital of appropriate symmetry, resulting in the formation of an agostic bond (intramolecular case) or an adduct (σ complex, intermolecular case). The second step, insertion, involves back-donation from an occupied metal-based orbital to a C−H antibonding σ^*_{CH} orbital, resulting in metal alkyl hydride formation. Back-donation to σ^*_{CH} should be significant in order to cause C−H oxidative addition, otherwise agostic complexes[25] or σ complexes[9] are more stable than the corresponding insertion products. Recent theoretical[26] and experimental[1b−e] studies extensively support this model.

In both aromatic and aliphatic PC−Rh systems described in this work C−H oxidative addition takes place. The agostic η^2-C,H complexes in both cases are close in energy to the C−H oxidative addition TS (Schemes 4 and 5, Figures 1 and 2). These early TSs reflect that the intermediacy of agostic complexes

(24) Hoffmann, R.; Saillard, J. Y. *J. Am. Chem. Soc.* **1984**, *106*, 2006. See also: Low, J. J.; Goddard, W. A. *J. Am. Chem. Soc.* **1986**, *108*, 6115.
(25) For reviews on agostic complexes, see: (a) Brookhart, M.; Green, M. L. H.; Wong, L.-L. *Prog. Inorg. Chem.* **1988**, *36*, 1. (b) Crabtree, R. H. *Angew. Chem., Int. Ed. Engl.* **1993**, *32*, 789.
(26) (a) Niu, S.; Hall, M. B. *Chem. Rev.* **2000**, *100*, 353. See also: (b) Cundari, T. *J. Am. Chem. Soc.* **1994**, *116*, 340. (c) Musaev, D. G.; Morokuma, K. *J. Am. Chem. Soc.* **1995**, *117*, 799. (d) Margl, P.; Ziegler, T.; Bloechl, P. E. *J. Am. Chem. Soc.* **1995**, *117*, 12625. (d) Siegbahn, P. E. M. *J. Am. Chem. Soc.* **1996**, *118*, 1487.

promotes C−H oxidative addition in both aliphatic and aromatic case. This is despite the differences in η^2-C,H bonding, indicating that back-donation to the σ^* orbital of η^2-C,H bond is sufficient for oxidative addition to occur in both aromatic and aliphatic PC−Rh cases and the relatively low electron density of the $[Rh(PR_3)(MeOH)_2]^+$ fragment is adequate for C−H oxidative addition. In the aromatic system the pattern of agostic interactions and C−H oxidative addition is relatively simple. We could not find a direct C−H activation pathway starting from η^2-C,C arene π-bound complex. In all cases the aromatic C−H oxidative addition was found to proceed through agostic intermediates. Interestingly, our computational results indicate that *the formation of η^2-C,C π-complex is not essential for the aromatic C−H oxidative addition*, similarly to several reported cases of intermolecular[6] or intramolecular[7] C−H activation. It should be noted that chelation in the PC−Rh system can impose certain geometric restrictions on the possible modes of metal−substrate interaction.[7] However, the optimized geometries of both η^2-C,H and η^2-C,C complexes, **7** and **8**, respectively, do not show significant strain and are almost equivalent energetically. Importantly, when in computational studies we attempted to detect a direct C−H activation pathway starting from the η^2-C,C π complex, agostic species preceding C−H oxidative addition were consistently found. It was reported that activation of vinylic C−H in ethylene bound to a Cp*Ir-(PMe_3) fragment proceeds not through an η^2-C,C π-complex intermediate but through a C−H σ complex.[27] Aromatic C−H oxidative addition may proceed not only through η^2-C,C arene π complex but also directly through a C−H σ complex.[6] It has been reported that an η^2-C,C complex appears to be the most energetically stable intermediate in the course of C−H oxidative addition of benzene by a cationic Pt(II) complex; however, it was proposed that this π complex rearranges into a η^2-C,H one, which is essential for C−H activation.[4] It is likely that, in most cases of arene C−H oxidative addition, η^2-C,C π-bonding may bring the arene into the vicinity of the metal, and the resulting π complex leads to the η^2-C,H bonding necessary for C−H activation. It is also possible that C−H oxidative addition takes place directly through a C−H σ complex, the π complex being a resting state, as we found in the Rh−PC system. In any case, η^2-C,H seems to be essential for arene C−H oxidative addition.

In the aliphatic PC−Rh system, the wide range of bonding possibilities and the lack of symmetry result in a complex pattern of agostic interactions. Thus, *complex* **2c** *demonstrates various types of C−H coordination occurring in one species.* Moreover, *the agostic interactions control the reversible C−H oxidative addition in the system, leading to energetically distinct C−H activation processes, which are observed experimentally and confirmed in the computational study*. η^2-C,H bonding was suggested to play a critical role in alkane C−H bond activation.[1] Regarding the simplest alkane molecule, methane, theoretical calculations predict various modes of methane coordination including η^2-C,H, η^2-H,H, and η^3-H,H,H interactions[9,26] and methane rotation involving alternating η^2-C,H bonds.[28] It should be noted that the involvement of an additional C−H bond in the interaction with the metal center in the agostic intermediate **12*** is weak, far from being a true η^2-H,H or η^3-H,C,H one. It should be considered rather a geometric predisposition[29] of a specific C−H to η^2-C,H bonding, imposed by η^2-C,H coordination of the other C−H bond. This weak interaction, however, can control the C−H oxidative addition pattern. It suggests that the overall influence of C−H bond coordination on C−H oxidative addition may be more complex than expected.

Table 3. Activation Parameters for C−H Reductive Elimination at the mPW1k/SDB-cc-pVDZ//mPW1k/SDD Level of Theory

	$\Delta G^{\ddagger}$ (kcal/mol)	$\Delta H^{\ddagger}$ (kcal/mol)	$\Delta S^{\ddagger}$ (eu)
benzyl−PC/Rh-*endo*	9.1	8.3	−2.5
benzyl−PC/Rh-*exo*	12.7	12.1	−2.0
aryl−PC/Rh	4.5	4.3	−0.7

As the C−H reductive elimination is concerned, both aryl-H and benzyl-H reductive elimination processes are characterized by comparable small negative activation entropies (Table 3), whereas the enthalpies are different. Benzylic C−H reductive elimination is expected to be more facile than arene C−H reductive elimination (M−benzyl bond is weaker than M−aryl). In addition, five-membered rings (aromatic PC−Rh) are at least as stable as six-membered ones (aliphatic PC−Rh). It is surprising, therefore, that in our PC systems there is an opposite trend for aryl-H vs benzyl-H reductive elimination. Factors other than M−C bond strength may be involved in controlling the relative rates of the reductive elimination. One of the factors may be the higher directionality of the sp^3-hybridized benzylic C−M bond vs sp^2 aryl C−M bond. However, as the activation entropies for the reductive elimination in both systems are comparable, the directionality of the bonds does not appear to play a significant role. We suggest the following explanation. The products of the reductive elimination, i.e., the agostic complexes, both in the aromatic and aliphatic cases, are very close in energy to the transition state, which is a late transition state regarding reductive elimination. Thus, formation of a strong aryl C−H bond and better metal η^2-C−H bonding in the aryl agostic intermediate correlates with a lower energy TS and can explain the lower activation enthalpy in the aromatic case. Formation of stronger Rh−C_{aryl} bond resulting in acidification of the C−H proton, and its scrambling by the metal center can also account for the observed lower activation barrier in the aryl−PC system (vide infra).

***η^2*-C,H Bond Coordination in Electrophilic vs Nucleophilic Arene C−H Bond Activation: Agostic C−H Bond Acidity and C−H Bond Oxidative Addition.** It is generally recognized that the coordination of a C−H bond to a metal can result in its enhanced acidity due to the donation from the C−H σ orbital to the metal. A number of recent examples indicate that arene C−H agostic bonding may result in a C−H acidity high enough to show exchange with water and deprotonation with amines.[8] Thus, arene C−H σ complexes with late transition metals demonstrate that such bonding may alter the properties of the C−H bond to an extent resembling insertion of a heteroatom into it. Interestingly, the agostic complex **7** can be viewed as the one demonstrating both oxidative addition (nucleophilic metal insertion into a C−H bond) and electrophilic (H/D exchange due to the C−H bond acidity) reactivity patterns. Analysis by Cundari of experimental and theoretical reaction

(27) Stoutland, P. O.; Bergman R. G. *J. Am. Chem. Soc.* **1988**, *110*, 5732.
(28) (a) Martin. R. L. *J. Am. Chem. Soc*. **1999**, *121*, 9459. (b) Iron, M. A.; Lo, H. C.; Martin, J. M. L.; Keinan, E. *J. Am. Chem. Soc*. **2002**, *124*, 7041.
(29) For an example of a weak agostic bond as a result of geometric predisposition, see: Cooper, A. C.; Clot, E.; Huffman, J. C.; Streib, W. E.; Maseras, F.; Eisenstein, O.; Caulton, K. G. *J. Am. Chem. Soc.* **1999**, *121*, 97.

coordinates in oxidative addition reactions involving low-valent metals complexes and in σ-bond metathesis reactions involving high-valent ones revealed that there is a good degree of similarity between C−H activation mechanisms in both cases, early on in the reaction coordinate.[26b] Cationic metal centers were shown to form strong η^2 C−H σ bonds, due to the enhanced forward electron donation from the C−H σ orbital to the empty metal orbital.[1] As a consequence, they are expected to increase C−H bond acidity. When this electron donation is high enough, an electrophilic mechanism may operate, i.e., H^+ is expelled or abstracted by a base. In case of sufficient back-donation from a metal to C−H σ* orbital, oxidative addition takes place. Significantly, complex **4** demonstrates both types of C−H activation occurring concurrently. *Once a σ complex is formed, both electrophilic and nucleophilic (oxidative addition) mechanisms may be operating.* The question of the inherent nature of C−H activation remains a challenge to answer in some systems.[30] On the basis of our combined experimental and computational study, it might be envisaged that both electrophilic and oxidative addition mechanisms may be operating in the C−H bond activation by cationic metal centers, depending on the interplay between forward and back-donation upon C−H bond coordination.

Conclusions

Our combined experimental and theoretical study presents a comparison of C−H bond activation/reductive elimination in aliphatic and aromatic PC−Rh systems. The agostic interactions in the aliphatic case create a complex reactivity pattern due to multiple bonding possibilities. Upon formation of an arene agostic C−H bond it becomes sufficiently acidic to promote H/D exchange with water and alcohols. This was utilized in an unprecedented catalytic process in which the vinylic hydrogens of terminal olefins were selectively exchanged with deuterium using D_2O or MeOD as deuterium donors. The aromatic PC system demonstrates both nucleophilic (oxidative addition) and electrophilic (H/D exchange) type of C−H activation, while the aliphatic PC−Rh system shows only nucleophilic C−H activation by oxidative addition, which is a function of the different agostic interactions in the two systems. Thus, strong C−H bond precoordination was shown to be critical for both electrophilic and nucleophilic mechanisms of C−H activation *in the same system* (aryl PC/Rh). It suggests that fine-tuning of the electron density of the metal center and the reaction media can be utilized for selective C−H activation by various mechanisms, as exemplified in the reported selective deuteration of olefins.

Experimental Methods

General Methods. All experiments with metal complexes and the phosphine ligand were carried out under an atmosphere of purified nitrogen in an MBraun MB 150B-G glovebox. The complex $[Rh(coe)_2Cl]_2$ was prepared according to a literature procedure.[31]

^1H, ^{13}C, and ^{31}P NMR spectra were recorded at 400, 100, and 162 MHz, respectively, at 295 K, using a Bruker Avance-400 NMR spectrometer. ^1H NMR and $^{13}C\{^1H\}$ NMR chemical shifts are reported in ppm downfield from tetramethylsilane. ^1H NMR chemical shifts are referenced to the residual hydrogen signal of the deuterated solvents, and in $^{13}C\{^1H\}$ NMR the ^{13}C signal of the deuterated solvents was used as a reference. ^{31}P NMR chemical shifts are reported in ppm downfield from H_3PO_4 and referenced to an external 85% solution of phosphoric acid in D_2O. Saturation transfer experiments were performed by selective saturation of the hydride resonance. The response of the signal of the methylene protons was detected by comparison (difference spectrum) with a control experiment, in which the signal free area was irradiated under the same conditions. Abbreviations used in the description of NMR data are as follows: Ar, aryl; br, broad; dist, distorted; s, singlet; d, doublet; m, multiplet.

Electrospray (ES) mass spectrometry was performed at the Weizmann Institute of Science using a MicroMass LCZ Detector 4000 with CV = 43 V, temperature = 150 °C, and EE = 4.2 V. Elemental analysis was performed at Mikroanalytisches Laboratorium, 45470 Mülheim, Germany.

Preparation of Ligand 3. An acetone solution (75 mL) of $^tBu_2PH$ (4.42 g, 30.276 mmol) was added in a glovebox to an acetone solution (75 mL) of $PhCH_2Br$ (4.134 g, 25.23 mmol). The reaction mixture was refluxed under argon for 8 h, and then 150 mL of pentane was added, resulting in precipitation. The solid was collected, washed with pentane, and dissolved in 100 mL of degassed H_2O. An aqueous solution (100 mL) of NaOAc (25 g) was added, and the resulting solution was extracted with ether. The resulting colorless etheral solution was dried over Na_2SO_4 and filtered, and the solvent was removed under vacuum. The compound was further purified by distillation at 0.4 mm/Hg, bp 96−100 °C, resulting in 4.30 g (75% yield) of **1** as a viscous colorless liquid.

$^{31}P\{^1H\}$ NMR ($CDCl_3$): 36.06 (s). ^1H NMR ($CDCl_3$): 7.35−7.30 (m, 2H, Ar-*H*), 7.25−7.19 (m, 2H, Ar-*H*), 7.13−7.07 (m, 1H, Ar-*H*), 2.83 (d, $^2J_{PH}$ = 3.2 Hz, 2H, Ar−CH_2–P), 1.12 (d, $^3J_{PH}$ = 10.9 Hz, 18H, P−C(CH_3)$_3$. $^{13}C\{^1H\}$ NMR ($CDCl_3$): 141.58 (d, J_{PC} = 10.2 Hz, C_{ipso}, Ar), 129.50 (d, J_{PC} = 8.4 Hz, Ar), 128.18 (s, Ar), 125.24 (br s, Ar), 31.75 (d, $^1J_{PC}$ = 21.8 Hz, P−*C*(CH$_3$)$_3$), 29.71 (d, $^2J_{PC}$ = 13.0 Hz, P−C(*C*H$_3$)$_3$), 28.41 (d, $^1J_{PC}$ = 23.2 Hz, Ar−*C*H$_2$–P). The assignment of the signals in $^{13}C\{^1H\}$ NMR is confirmed by ^{13}C DEPT-135 NMR.

Reaction of $[Rh(coe)_2(solv)_n]BF_4$ with Ligand 1. Formation of the C−H Activation Products 4a−c. A THF (3 mL) solution of $AgBF_4$ (24 mg, 0.124 mmol) was added to a THF solution (4 mL) of $[Rh(coe)_2Cl]_2$ (44 mg, 0.062 mmol). Immediate precipitation of AgCl took place, which was removed by filtration after allowing the mixture to stand at room temperature for 15 min, resulting in a clear orange solution of **[**$Rh(coe)_2(THF)_n]BF_4$. A THF (3 mL) solution of ligand **1** (30 mg, 0.128 mmol) was added to this solution, resulting in color change to orange-red. The resulting mixture was kept at room temperature for 1 h followed by solvent evaporation under vacuum. The residue was washed with pentane and dissolved in 3 mL of MeOH, resulting in colorless solution. After keeping the solution for 1 h at room temperature, the solvent was evaporated under vacuum and the residue was then redissolved in either THF, methanol, or acetone, to yield quantitatively the corresponding solvento-complexes **4a**−**c**.

Complex 4a. $^{31}P\{^1H\}$ NMR (acetone-d_6): 111.35 (d, $^1J_{RhP}$ = 171.8 Hz). ^1H NMR (acetone-d_6): 7.36 (br s, 1H, Ar-*H*), 7.01 (br d, J_{HH} = 4.3 Hz, 1H, Ar-*H*), 6.82 (br m, 1H, Ar-*H*), 6.77 (dist t, J_{HH} = 4.3 Hz, 1H, Ar-*H*), 3.25 (br dd, $^2J_{HH}$ = 15.4 Hz, $^2J_{PH}$ = 10.2 Hz, 1H, Ar−CH_2−P, left part of AB system), 3.06 (br dd, $^2J_{PH}$ = 10.0 Hz, 1H, Ar−CH_2–P, right part of AB system), 1.36 (d, $^3J_{PH}$ = 13.6 Hz, 9H, P−C(CH_3)$_3$), 1.27 (d, $^3J_{PH}$ = 13.2 Hz, 9H, P−C(CH_3)$_3$), −22.41 (dd, $^1J_{RhH}$ = 34.5 Hz, $^2J_{PH}$ = 24.1 Hz, 1H, Rh−*H*). $^{13}C\{^1H\}$ NMR (acetone-d_6): 150.90 (br d, $^1J_{RhC}$ = 32.7 Hz, C_{ipso}−Rh), 149.58 (s, Ar), 149.48 (s, Ar), 135.02 (br s, Ar), 124.99 (s, Ar), 123.97 (br s, Ar), 36.21 (d, $^1J_{PC}$ = 17.2 Hz, P−*C*(CH$_3$)$_3$), 35.72 (d, $^1J_{PC}$ = 27.4 Hz, P−*C*(CH$_3$)$_3$), 33.55 (br d, $^1J_{PC}$ = 33.7 Hz, Ar−*C*H$_2$−P), P−C(*C*H$_3$)$_3$ signals overlapped with the signals of the solvent.

Complex 4b. $^{31}P\{^1H\}$ NMR (THF-d_8): 109.82 (br d, $^1J_{RhP}$ = 176.6 Hz). ^1H NMR (THF-d_8): 7.33 (br d, J_{HH} = 6.9 Hz, 1H, Ar-*H*), 6.92 (br d, J_{HH} = 7.7 Hz, 1H, Ar-*H*), 6.81 (m, 2H, Ar-*H*), 3.08 (dd, $^2J_{HH}$ =

(30) For two recent examples, see: (a) Zhong, H. A.; Labinger, J. A.; Bercaw, J. E. *J. Am. Chem. Soc.* **2002**, *124*, 1378. (b) Tellers, D. M.; Yung, C. M.; Arndtsen, B. A.; Adamson, D. R.; Bergman, R. G. *J. Am. Chem. Soc.* **2002**, *124*, 1400.

(31) Herde, J. L.; Senoff, C. V. *Inorg. Nucl. Chem. Lett.* **1971**, *7*, 1029.

16.6 Hz, $^2J_{PH}$ = 9.8 Hz, 1H, Ar−CH_2–P, left part of AB system), 3.06 (dd, $^2J_{PH}$ = 9.6 Hz, 1H, Ar−CH_2−P, right part of AB system), 1.37 (d, $^3J_{PH}$ = 13.7 Hz, 9H, P−C(CH_3)$_3$), 1.22 (d, $^3J_{PH}$ = 13.3 Hz, 9H, P−C(CH_3)$_3$), −24.07 (br s, 1H, Rh−*H*). ^{13}C{^{1}H} NMR (THF-d_8): 150.23 (m, C_{ipso}−Rh, Ar), 135.28 (s, Ar), 125.10 (s, Ar), 123.95 (s, Ar), 123.71 (s, Ar), 123.55 (s, Ar), 36.29 (d, $^1J_{PC}$ = 16.9 Hz, P−*C*(CH$_3$)$_3$), 35.42 (d, $^1J_{PC}$ = 26.9 Hz, P−*C*(CH$_3$)$_3$), 33.98 (br d, $^1J_{PC}$ = 33.8 Hz, Ar−*C*H$_2$−P), 30.14 (m, P−C(*C*H$_3$)$_3$), 29.44 (br s, P−C(*C*H$_3$)$_3$).

Complex 4c. ^{31}P{^{1}H} NMR (methanol-d_4): 109.82 (br d, $^1J_{RhP}$ = 175.8 Hz). ^{1}H NMR (methanol-d_4): 7.43 (br d, J_{HH} = 7.3 Hz, 1H, Ar-*H*), 6.98 (br d, J_{HH} = 7.2 Hz, 1H, Ar-*H*), 6.82 (m, 2H, Ar-*H*), 3.25 (ddd, $^2J_{HH}$ = 16.7 Hz, $^2J_{PH}$ = 10.2 Hz, $^3J_{RhH}$ = 2.2 Hz, 1H, Ar−CH_2−P, left part of AB system), 3.06 (dd, $^2J_{PH}$ = 9.9 Hz, 1H, Ar−CH_2–P, right part of AB system), 1.33 (d, $^3J_{PH}$ = 13.6 Hz, 9H, P−C(CH_3)$_3$), 1.21 (d, $^3J_{PH}$ = 13.0 Hz, 9H, P−C(CH_3)$_3$), −22.66 (dd, $^1J_{RhH}$ = 33.2 Hz, $^2J_{PH}$ = 26.5 Hz, 1H, Rh−*H*). ^{13}C{^{1}H} NMR (methanol-d_4): 150.40 (br d, $^1J_{RhC}$ = 36.8 Hz, C_{ipso}−Rh), 150.25 (m, Ar), 135.41 (s, Ar), 135.16 (s, Ar), 125.35 (m, Ar), 124.02 (m, Ar), 36.23 (d, $^1J_{PC}$ = 17.0 Hz, P−*C*(CH$_3$)$_3$), 35.48 (d, $^1J_{PC}$ = 27.6 Hz, P−*C*(CH$_3$)$_3$), 34.28 (br. d, $^1J_{PC}$ = 34.1 Hz, Ar−*C*H$_2$−P), 30.09 (m, P−C(*C*H$_3$)$_3$), 29.33 (br s, P−C(*C*H$_3$)$_3$).

ES MS positive mode (*m*/*e*): calcd for $C_{16}H_{29}OPRh$ (one MeOH molecule remains coordinated) MH^+, 371.28; found MH^+, 371.12. ES MS negative mode (*m*/*e*): calcd for BF_4, 86.80; found, 86.91.

Anal. Calcd for $C_{16}H_{29}OPRh$ (assuming one MeOH molecule remains coordinated): C, 41.95; H, 6.38. Found: 41.93; 6.44.

Deuteration Experiments. In a typical experiment, complex **4** (15 mg, 0.040 mmol) was dissolved in a solvent of choice (CD_3OD or acetone/D_2O (5:1 v/v) mixture). Styrene (about 70 equiv) was added to the solution of **4**, and the resulting mixture was placed in the screw-cap NMR tube and was heated for 24 h at 65 °C. Toluene-d_8 (20 μL) was added to the reaction mixture as a standard, and the integrals of the signals of vinylic deuterons in ^{2}D NMR were compared to those of tolune-d_8. In all the cases exclusive vinylic deuteration was observed. Formation of styrene-d_3 was confirmed by GC-MS.

Computational Methods

All calculations were carried out using the Gaussian 98 program revision A.11[32] running on Compaq ES40 and XP1000 workstations as well as on a mini-farm of Pentium IV Xeon 1.7/2.0 GHz PC's running Red Hat Linux 7.2 in our group, on an experimental Linux PC Farm at the Faculty of Physics, and on the (Israel) Inter-University Computing Center (IUCC) SGI Origin 2000.

The mPW1k (modified Perdew−Wang 1-parameter for kinetics) exchange-correlation functional of Truhlar and co-workers[33] was employed in conjunction with the SDD and SDB-cc-pVDZ basis sets (see below). The mPW1k functional was very recently shown[28b,33,34] to yield more reliable reaction barrier heights than other exchange-correlation functionals.

The SDD basis set is the combination of the Huzinage−Dunning double-ζ basis set on lighter elements with the Stuttgart−Dresden basis set−relativistic effective core potential (RECP) combination[35] on the transition metals. The SDB-cc-pVDZ basis set combines the Dunning cc-pVDZ basis set[36] on the main group elements with the Stuttgart−Dresden basis set-RECP combination[35] on the transition metals, with an *f*-type polarization exponent taken as the geometric average of the two *f*-exponents given in the Appendix to ref 37.

Geometry optimizations for minima were carried out using the standard Schlegel algorithm[38] in redundant internal coordinates until in the neighborhood of the solution and then continued using analytical second derivatives.[39] Optimizations for transition states were carried out by means of the QST3 approach,[40] with an initial guess for the transition state being generated from manual manipulation of the geometry using MOLDEN.[41] In cases where this approach failed to converge, we used analytical second derivatives at every step.

Zero-point and RRHO (rigid rotor−harmonic oscillator) thermal corrections (to obtain ΔS, ΔH, and ΔG values) were obtained from the unscaled computed frequencies.

Where necessary, the Grid = UltraFine combination, i.e., a pruned (99 590) grid in the integration and gradient steps and a pruned (50 194) grid in the CPKS (coupled perturbed Kohn−Sham) steps, was used as recommended in ref 42.

Zero-point and RRHO (rigid rotor−harmonic oscillator) thermal corrections were obtained from the unscaled computed frequencies.

Where necessary to resolve ambiguities about the nature of a transition state, intrinsic reaction coordinate (IRC[43]) calculations were carried out. In some cases where IRC calculation failed for technical reason, displacements were made along the normal coordinate for the imaginary frequencies and optimizations started from there. While this pseudo-IRC procedure is less unambiguous than IRC, it at least offers some form of corroboration.

For interpretative purposes, atomic partial charges and Wiberg bond indices[44] were obtained by means of a natural population analysis (NPA)[45] at the mPW1k/SDD level.

The energetics for our final reaction profile were validated by single-point energy calculations, using the mPW1k/SDD reference geometries, at the higher level of theory mPW1k/SDB-cc-pVDZ.

Acknowledgment. This work was supported by the Israel Science Foundation (Grant No 83/00), the MINERVA foundation, Munich, Germany, the Tashtiyot program of the Ministry of Science (Israel), the Israel Inter-University Computing Center, and the Helen and Martin Kimmel Center for Molecular Design. We thank Dr. Leonid Konstantinovsky for the help with NMR measurements. D.M. holds the Israel Matz Professorial Chair in Organic Chemistry. J.M.L.M. is a member of the Lise Meitner-Minerva Center for Computational Quantum Chemistry.

Supporting Information Available: *XYZ* coordinates of all computed structures and SST spectrum of complex **4b** (PDF). This material is available free of charge via the Internet at http://pubs.acs.org.

JA029197G

(32) Frisch, M. J.; Trucks, G. W.; Schlegel, H. B.; Scuseria, G. E.; Robb, M. A.; Cheeseman, J. R.; Zakrzewski, V. G.; Montgomery, J. A., Jr.; Stratmann, R. E.; Burant, J. C.; Dapprich, S.; Millam, J. M.; Daniels, A. D.; Kudin, K. N.; Strain, M. C.; Farkas, O.; Tomasi, J.; Barone, V.; Cossi, M.; Cammi, R.; Mennucci, B.; Pomelli, C.; Adamo, C.; Clifford, S.; Ochterski, J.; Petersson, G. A.; Ayala, P. Y.; Cui, Q.; Morokuma, K.; Salvador, P.; Dannenberg, J. J.; Malick, D. K.; Rabuck, A. D.; Raghavachari, K.; Foresman, J. B.; Cioslowski, J.; Ortiz, J. V.; Baboul, A. G.; Stefanov, B. B.; Liu, G.; Liashenko, A.; Piskorz, P.; Komaromi, I.; Gomperts, R.; Martin, R. L.; Fox, D. J.; Keith, T.; Al-Laham, M. A.; Peng, C. Y.; Nanayakkara, A.; Challacombe, M.; Gill, P. M. W.; Johnson, B.; Chen, W.; Wong, M. W.; Andres, J. L.; Gonzalez, C.; Head-Gordon, M.; Replogle, E. S.; Pople, J. A. *Gaussian 98*, revision A.11; Gaussian, Inc.: Pittsburgh, PA, 2001.
(33) Lynch, B. J.; Fast, P. L.; Harris, M.; Truhlar, D. G. *J. Phys. Chem. A* **2000**, *104*, 4811
(34) (a) Parthiban, S.; de Oliveira, G.; Martin, J. M. L. *J. Phys. Chem. A* **2001**, *105*, 895. (b) Lynch, B. J.; Truhlar, D. G. *J. Phys. Chem. A* **2001**, *105*, 2936.
(35) Dolg, M. In *Modern Methods and Algorithms of Quantum Chemistry*; Grotendorst, J., Ed.; John von Neumann Institute for Computing: Jülich, Germany, 2000; Vol. 1, pp 479−508.
(36) Dunning, T. H., Jr. *J. Chem. Phys.* **1989**, *90*, 1007.
(37) Martin, J. M. L.; Sundermann, A. *J. Chem. Phys.* **2001**, *114*, 3408.
(38) Schlegel, H. B. *J. Comput. Chem.* **1982**, *3*, 214. Peng, C.; Ayala, P. Y.; Schlegel, H. B.; Frisch, M. J. *J. Comput. Chem.* **1996**, *17*, 49.
(39) Stratmann R. E.; Burant J. C.; Scuseria G. E.; Frisch M. J. *J. Chem. Phys.* **1997**, *106*, 10175.
(40) Peng, C.; Schlegel, H. B. *Isr. J. Chem.* **1994**, *33*, 449.
(41) Schaftenaar, G. Molden 3.6, 1999. URL: http://www.cmbi.kun.nl/~schaft/molden/molden.html.
(42) Martin, J. M. L.; Bauschlicher, C. W.; Ricca, A. *Comput. Phys. Commun.* **2001**, *133*, 189.
(43) Gonzalez, C.; Schlegel, H. B. *J. Chem. Phys.* **1989**, *90*, 2154; *J. Phys. Chem.* **1990**, *94*, 5523.
(44) Wiberg, K. B. *Tetrahedron* **1968**, *24*, 1083.
(45) Reed, A. E.; Curtiss, L. A.; Weinhold, F. *Chem. Rev.* **1988**, *88*, 899.